Global stability analysis of slat noise mechanisms

Smail Lebbal, Maxime Huet, Samir Beneddine, Cédric Content, Denis Sipp

GLOBAL STABILITY ANALYSIS OF SLAT NOISE MECHANISMS

Smail Lebbal
DAAA, ONERA, Université Paris Saclay, F-92322 Châtillon - France
e-mail: smail.lebbal@onera.fr
Maxime Huet
DAAA, ONERA, Université Paris Saclay, F-92322 Châtillon - France
email: maxime.huet@onera.fr
Samir Beneddine
DAAA, ONERA, Université Paris Saclay, F-92322 Meudon - France
email: samir.beneddine@onera.fr
Cédric Content
DAAA, ONERA, Université Paris Saclay, F-92322 Châtillon - France
email: cedric.content@onera.fr
Denis Sipp
DAAA, ONERA, Université Paris Saclay, F-92322 Meudon - France
email: denis.sipp@onera.fr

The present work studies the mechanism of tonal slat noise generation in high-lift devices. Peaks in the emitted noise spectrum are observed for small-scale geometries with various slat configurations. They are attributed to a feedback mechanism in the slat cove similar to that in cavity flows. The objective of this study is to characterize the flow structures which are at the origin of this tonal noise, and future work may focus on investigating the effect of the flow parameters (Reynolds number, Mach number, angle of attack) on its generation. To this end, a 2-element airfoil composed of a slat and a main body is considered. This geometry is designed to isolate slat noise from other possible sources while providing a flow representative of a realistic 3-element airfoil near the slat. The coherent structures involved in the tonal noise are then identified from high-fidelity unsteady CFD data using Spectral Proper Orthogonal Decomposition (SPOD). The present work reveals that the obtained structures show good agreement with the recent paper of Himeno et al. (JFM 2021). In addition to the midrange frequencies, which are classically associated with the loop feedback mechanism, the analysis also reveals a high-frequency mode whose structure is concentrated in the wake of the upper slat trailing edge.
Keywords: slat noise, SPOD, global stability.

1. Introduction

The limits of aircraft noise reduction techniques are constantly being pushed back as a direct consequence of the enhanced understanding of noise generation mechanisms. In this vein, we propose studying the tonal slat noise mechanism with a method that combines high-fidelity and low-fidelity models. These methods consist of a resolvent analysis of the mean flow that allows identifying the most amplified coherent structures of the flow [1], and Spectral Proper Orthogonal Decomposition (SPOD) analysis to extract

energetic coherent structures from unsteady experimental or high-fidelity CFD data [2]. Note that several studies have established the link between these two approaches by showing that the optimal mode of the resolvent analysis is qualitatively similar to the dominant SPOD mode in the presence of a strong instability mechanism (see, for instance, [3]). Therefore, as a first step in investigating the origin of tonal slat noise, the present work focuses on the SPOD analysis.

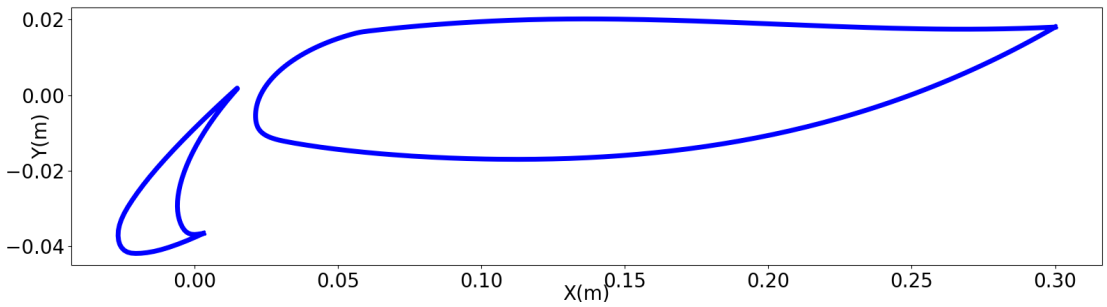

Figure 1: Illustration of the high-lift airfoil geometry.

To isolate the slat noise sources, we use the 2-element airfoil proposed by Terracol *et al.* [4] and illustrated in figure (1). This airfoil is derived from the 3-element FNG Airbus geometry airfoil, developed in the German Research & Technology projects LuFo III and ProHMS and already used by DLR, see for instance [5]. In the 2-element airfoil, the slat and the leading edge of the main element are identical to the reference airfoil concerning the noise generated in the slat cove, while the flap is removed to get rid of its noise and reduce flow deviation. The final geometry is obtained by an optimization process, and the interested reader may refer to Terracol *et al.* [4] for further information.

The slat noise far-field power spectral density is illustrated in figure (2). In addition to the broadband component, we observe narrowband peaks. These peaks are usually attributed to the well-known aeroacoustic feedback mechanism presented by Rossiter [6] in his seminal paper. This mechanism involves the interaction between the perturbations generated at the slat's lower trailing edge and the acoustic waves generated by the impact of the shear layer on the slat surface. Recently, several authors [4, 7] extended Rossiter's model, initially developed for open cavity flows, to the flow around the slat cavity of a high-lift airfoil. These semi-empirical models involve the effect of the shear layer properties and the impingement location on the tones frequencies in contrast with the original Rossiter model.

The paper is organized as follows. First, a short presentation of the SPOD method is given. Then, the database extracted from a Lattice Boltzmann Method (LBM) simulation is described. Finally, the resulting SPOD modes are illustrated for relevant frequencies in the SPOD spectrum.

2. Spectral proper orthogonal decomposition

The spectral proper orthogonal decomposition seeks a mode base approximating a data set's coherent structures. In addition, the SPOD method characterizes spatiotemporal correlation in a flow field and, thus, yields spatiotemporal evolving modes (harmonic in time) in contrast with the classical space-only POD. A review of this method is given, for instance, in Schmidt & Colonius [8] and is summed up hereafter. The database of all available snapshots from the flow is organized as a matrix of the form $\mathbf{Q} = \left\{q^{(1)}, ..., q^{(N)}\right\} \in \mathbb{R}^{M\mathrm{x}N}$, with M the number of degrees of freedom and N the number of time steps. The SPOD modes are then the eigenvectors of the eigenvalue problem given, for each frequency f, by

$$\hat{\mathbf{S}}_f \mathbf{W} \hat{\mathbf{\Phi}}_f = \hat{\mathbf{\Phi}}_f \mathbf{\Lambda}_f, \quad \hat{\mathbf{\Phi}}_f \in \mathbb{C}^{M\mathrm{x}M}, \tag{1}$$

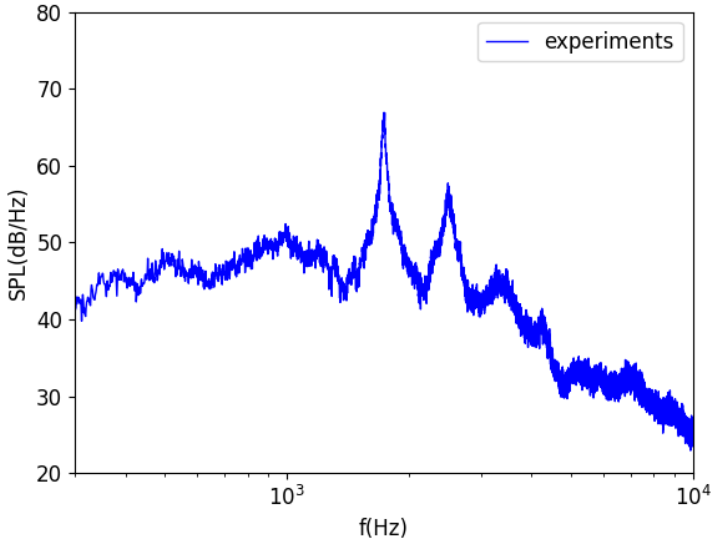

Figure 2: Far-field noise power spectral density (from Valiant project).

with $\hat{\mathbf{S}}$ the cross-spectral density (CSD) tensor. The resulting SPOD modes are orthonormal at each frequency in the norm $< \hat{q}_1, \hat{q}_2 >= \hat{q}_2^* \mathbf{W} \hat{q}_1$.

The cross-spectral density tensor expression may be found, for instance, in [2] as a function of the data fields for each frequency:

$$\hat{\mathbf{S}}_f = \frac{1}{Nb} \hat{\mathbf{Q}}_f \hat{\mathbf{Q}}_f^*. \tag{2}$$

where Nb is the number of realizations (number of blocks for Fourier transform) and $\hat{\mathbf{Q}}_f$ is the Fourier transformed data matrix at frequency f ($\hat{\mathbf{Q}}_f = \left\{ \hat{q}_f^{(1)}, ..., \hat{q}_f^{(Nb)} \right\} \in \mathbb{C}^{M \text{x} Nb}$).

In the case of high-fidelity data, this problem is often too large to solve. Instead, one may consider the vector $\hat{\mathbf{\Psi}}_f \in \mathbb{C}^{Nb \text{x} M}$ defined as $\hat{\mathbf{\Phi}}_f = \hat{\mathbf{Q}}_f \hat{\mathbf{\Psi}}_f$, leading to a smaller eigenvalue problem which depends directly on the data vectors.

$$\frac{1}{Nb} \hat{\mathbf{Q}}_f^* \mathbf{W} \hat{\mathbf{Q}}_f \hat{\mathbf{\Psi}}_f = \hat{\mathbf{\Psi}}_f \mathbf{\Lambda}_f. \tag{3}$$

As highlighted by Himeno *et al.* [9], using the classical scalar product based on the turbulent kinetic energy norm to define $\mathbf{W}$ is not well suited for studying acoustic radiation. Therefore, we use a simple weighted 2-Norm applied to the pressure field instead.

3. SPOD analyses

The database used in this study is extracted from an LBM simulation conducted by Airbus with the commercial code ProLB. The parameters of the simulation are: the Reynolds number based on the cord length $Re = 10^6$, the Mach number $Ma = 0.15$, and the incidence angle 25° between the airflow direction and the airfoil reference axis.

The database contains $Nt = 40\,000$ snapshots uniformly distributed in time over a physical duration of 0.2 s. Since our concern is the midrange frequencies (Rossiter's mechanism [4, 6]), the sampling frequency ($f_s = 100$ kHz) is taken large enough to minimize aliasing. Furthermore, as mentioned by several authors [4, 7, 9], the slat tonal noise generation mechanism is driven by 2-dimensional structures. Therefore, the dataset extracted corresponds to 2D plans in the crosswise direction. In addition, the

database includes 20 spanwise plans. These plans mainly ensure a statistical convergence by extending the number of flow realizations considered for the SPOD. We use a classical overlap of 50% between realizations as preconized by Schmidt & Colonius [8]. Table (1) summarizes the parameters of the SPOD study.

Signal	Sampling frequency	Number of segments	Overlap
0.2 s	100 kHz	140	0.5

Table 1: SPOD parameters.

The SPOD spectrum of the first mode is shown in figure (3a), together with the 99% confidence interval evaluated by following the approach from Schmidt & Colonius [8]. The narrowband peak frequencies observed in the far field are also identified in the SPOD spectrum. As for the far-field spectra, the most dominant frequencies are the second and the third Rossiter's frequencies. There is a fair agreement between the frequencies of the far-field tones and those in the SPOD spectrum (Table 2).

Mode	f_n SPOD	f_n experiments
$n = 1$	$f = 820$ Hz	$f = 860$ Hz
$n = 2$	$f = 1640$ Hz	$f = 1730$ Hz
$n = 3$	$f = 2420$ Hz	$f = 2480$ Hz
$n = 4$	$f = 3220$ Hz	$f = 3340$ Hz
$n = 5$	$f = 4080$ Hz	$f = 4247$ Hz

Table 2: Comparison between the tonal frequencies in th SPOD and far-field spectra.

To visualize the relative importance of the first SPOD mode over the lower-rank modes, we illustrate in figure (3b) the energy fraction of the first mode defined as $\lambda_1 / \sum \lambda_j$. It is found that the modes corresponding to the peaks observed in the SPOD spectrum strongly dominate for each frequency since they correspond to a relative energy fraction roughly between 65% and 95%.

The spatial structure of the five dominant modes in the spectrum is shown in figure (4). The first mode (f_1) is dominated by structures originating from the impingement of the vortices convected by the main shear layer on the slat surface. Then, the four next modes hint at a developing Kevin–Helmholtz instability in the mixing layer. Finally, the last mode is associated with high-frequency structures originating from the turbulence accelerated through the slat gap and the wake of the stat trailing edge. These coherent structures extracted with the SPOD method appear rather consistent with the results of Himeno *et al.* [9].

To give further insights, we show in figure (5) the spatial magnitude of the first SPOD mode on the same relevant frequencies as in the last paragraph. The midrange frequencies show that the most energetic structures are located in the zone of the impingement on the slat surface and the main shear layer. In contrast, the energy of the high-frequency mode is concentrated in the zone between the airfoil's leading edge and the trailing edge of the slat, consistent with the pressure spectra along the wake given by Terracol *et al.* [4].

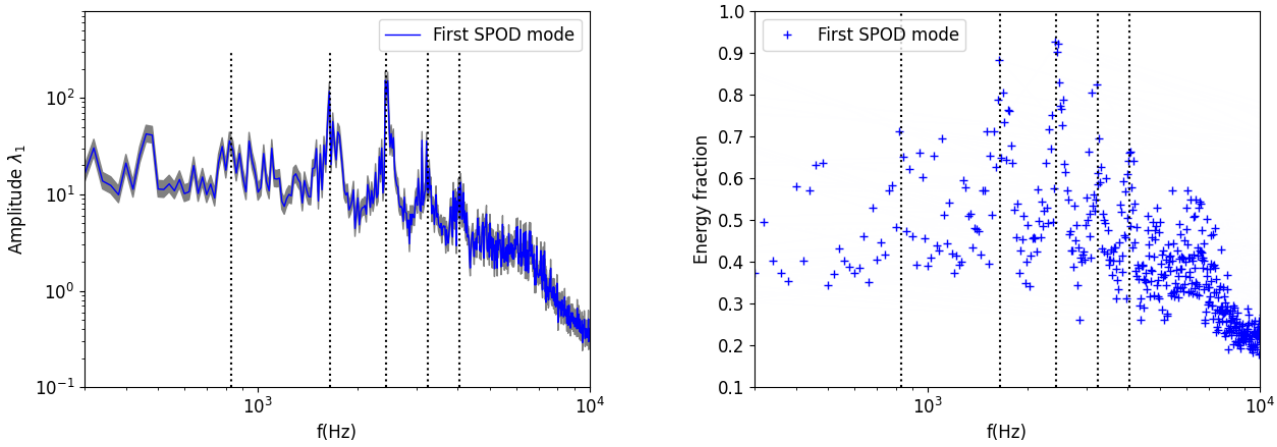

(a) Spectrum of the first SPOD mode.

(b) Energy fraction of the first SPOD mode.

Figure 3: Spectrum of the first SPOD mode, including the 99% confidence interval. The highlighted modes correspond to the peaks observed in the SPOD spectrum. The frequencies are $f_1 = 820$ Hz, $f_2 = 1640$ Hz, $f_3 = 2420$ Hz, $f_4 = 3220$ Hz, $f_5 = 4080$ Hz.

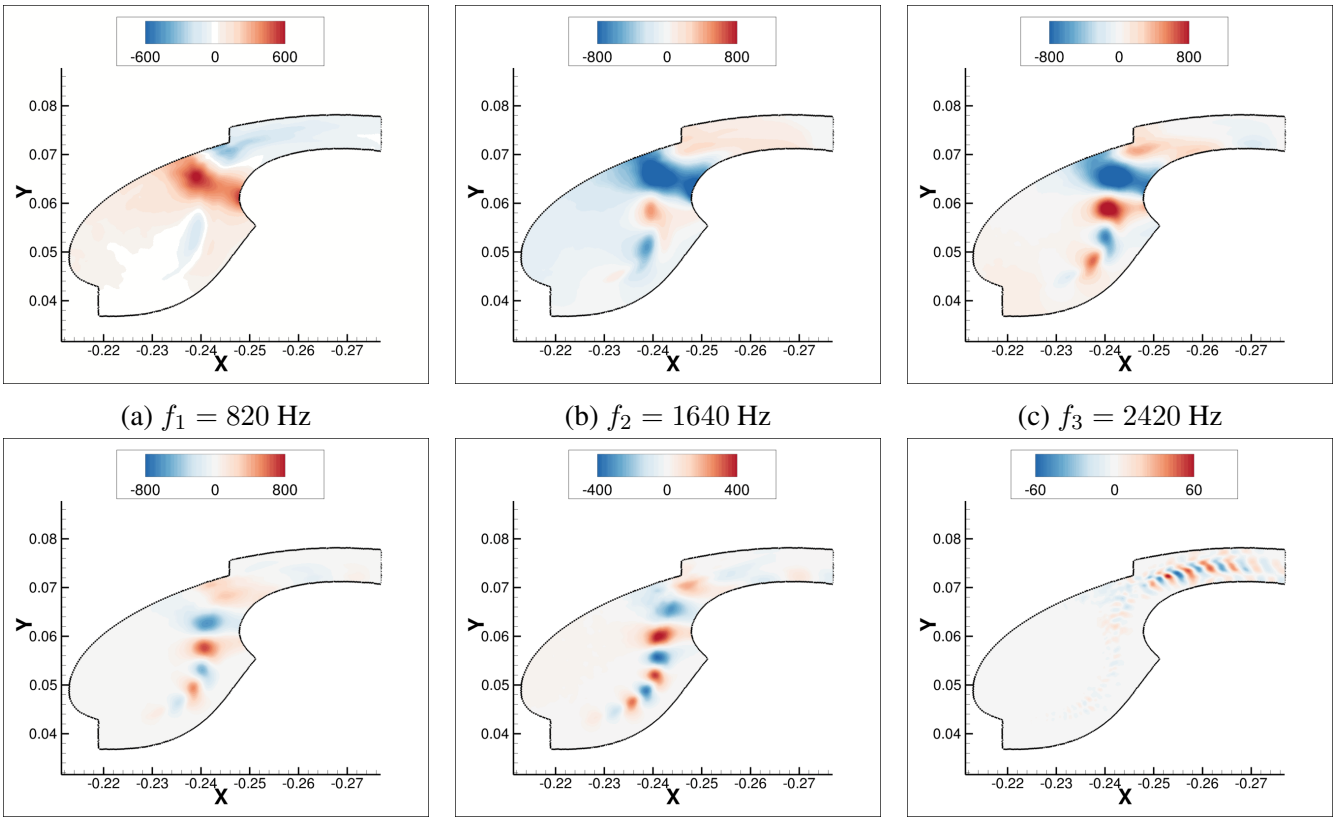

(a) $f_1 = 820$ Hz

(b) $f_2 = 1640$ Hz

(c) $f_3 = 2420$ Hz

(d) $f_4 = 3220$ Hz

(e) $f_5 = 4080$ Hz

(f) $f = 45520$ Hz

Figure 4: Real part of the first SPOD mode at the selected frequencies.

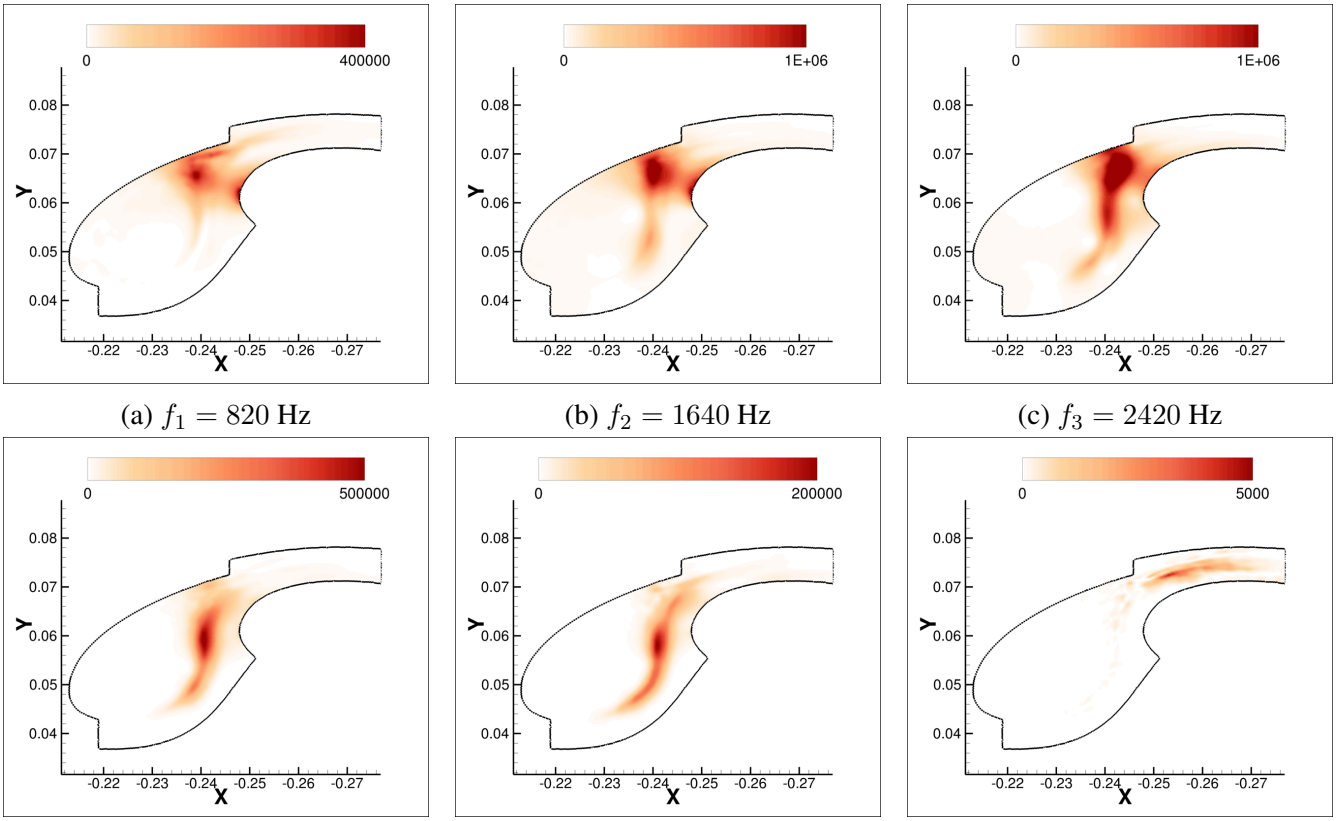

(a) $f_1 = 820$ Hz (b) $f_2 = 1640$ Hz (c) $f_3 = 2420$ Hz

(d) $f_4 = 3220$ Hz (e) $f_5 = 4080$ Hz (f) $f = 45520$ Hz

Figure 5: Magnitude of the first SPOD mode at the selected frequencies.

4. Conclusion and perspectives

In the present paper, we applied the SPOD method to investigate the tonal slat noise mechanism. The 2-element high lift airfoil chosen overcomes the spurious noise sources, especially the noise generation of the flap.

It is found that the main structures at the tonal frequencies are associated with Rossier's mechanism. In addition, a good agreement is found between the frequencies predicted by the SPOD method and those extracted from the experimental far-field spectrum. A high-frequency mode is also presented. This mode is dominated by the wake of the slat's upper trailing edge.

The result obtained by the SPOD decomposition, especially the dominance of the first SPOD mode over lower-ranked ones, indicates that these structures are likely to originate from instability mechanisms that may be further investigated through global stability and resolvent analyses. Moreover, as shown by several authors [2, 3], the spatial shape of the dominant resolvent mode is expected to be close to the dominant SPOD mode analyzed in this paper. Therefore, an extension of this study to global stability analysis is considered, together with data assimilation methods to tune the mean flow with experimental and high-fidelity numerical data. Furthermore, we aim to investigate with this low-order method the effect of the flow parameters (Reynolds number, Mach number, and angle of attack) on the slat noise generation mechanism.

Acknowledgments

This work was carried out in the framework of the MAMBO project, supported by the French Civil Aviation Agency (DGAC), the "France Relance" national recovery plan, and the "Nextgeneration EU" european recovery plan.

REFERENCES

1. Sipp, D., Marquet, O., Meliga, P. and Barbagallo, A. Dynamics and control of global instabilities in open-flow: a linearized approach, *Applied Mechanics Reviews*, **63**, 030801, (2010).

2. Towne, A., Schmidt, O. T. and Colonius, T. Spectral proper orthogonal decomposition and its relationship to dynamic mode decomposition and resolvent analysis, *Journal of Fluid Mechanics*, pp. 821–867, (2018).

3. Beneddine, S., Sipp, D., Arnault, A., Dandois, J. and Lesshafft, L. Conditions for validity of mean flow stability analysis, *Journal of Fluid Mechanics*, pp. 485–504, (2016).

4. Terracol, M., Manoha, E. and Lemoine, B. Investigation of the unsteady flow and noise generation in a slat cove, *AIAA Journal*, pp. 469–489, (2016).

5. Wild, J., Pollenske, M. P. and Nagel, B. An integrated design approach for low noise exposing high-lift devices, *Proc. 3rd AIAA Flow Control Conference, AIAA Paper 2006-2843*, (2016).

6. Rossiter, J. E. Wind tunnel experiments of the flow over rectangular cavities at subsonic and transonic speeds, *Ministry of Aviation; Royal Aircraft Establishment*, (1964).

7. Souza, D., Rodríguez, D., Himeno, F. and Medeiros, M. Dynamics of the large-scale structures and associated noise emission in airfoil slats, *Journal of Fluid Mechanics*, pp. 1004–1034, (2019).

8. Schmidt, O. and Colonius, T. Guide to spectral proper orthogonal decomposition, *AIAA Journal*, pp. 1023–1033, (2020).

9. Himeno, F., Souza, D., Amaral, F., Rodríguez, D. and Medeiros, M. SPOD analysis of noise-generating Rossiter modes in a slat with and without a bulb seal, *Journal of Fluid Mechanics*, pp. 1–24, (2021).